Applied Geochemistry 50 (2014) 53–65

Contents lists available at ScienceDirect

Applied Geochemistry

journal homepage: www.elsevier.com/locate/apgeochem

Evaluating the use of strontium isotopes in tree rings to record the isotopic signal of dust deposited on the Wasatch Mountains

Olivia L. Miller [a,*], Douglas Kip Solomon [a], Diego P. Fernandez [a], Thure E. Cerling [a,b], David R. Bowling [b]

[a] University of Utah, Geology & Geophysics, Frederick Albert Sutton Building, 115 S 1460 East Room 383, Salt Lake City, UT 84112, United States
[b] University of Utah, Department of Biology, 257 S 1400 E, Salt Lake City, UT 84112, United States

ARTICLE INFO

Article history:
Available online 27 August 2014
Editorial handling by M. Kersten

ABSTRACT

Dust cycling from the Great Basin to the Rocky Mountains is an important component of ecological and hydrological processes. We investigated the use of strontium (Sr) concentrations and isotope ratios ($^{87}Sr/^{86}Sr$) in tree rings as a proxy for dust deposition. We report Sr concentrations and isotope ratios ($^{87}Sr/^{86}Sr$) from atmospherically deposited dust, soil, bedrock, and tree rings from the Wasatch Mountains to investigate provenance of dust landing on the Wasatch Mountains and to determine if a dust Sr record is preserved in tree rings. Trees obtained a majority of their Sr from dust, making them a useful record of dust source and deposition. Dust contributions of Sr to soils were more than 94% over quartzite, 63% over granodiorite, and 50% over limestone. Dust contributions of Sr to trees were more than 85% in trees growing over quartzite, 55% over granodiorite, and between 0% and 92% over limestone. These findings demonstrate that a dust signal was preserved in some tree rings and reflects how Sr from dust and bedrock mixes within the soil. Trees growing over quartzite were most sensitive to dust. Changes in Sr isotope ratios for a tree growing over quartzite were interpreted as changes in dust source over time. This work has laid the foundation for using tree rings as a proxy for dust deposition over time.

1. Introduction

Wind erosion and dust emissions are important components of many ecological processes on local and global scales (Engelbrecht and Derbyshire, 2010; Field et al., 2009). Many soils in the American Southwest are covered in biological soil crusts that reduce the wind's ability to erode soils (Belnap and Gillette, 1997; Eldridge and Leys, 2003). However, human activity has disturbed some of these soils, resulting in increased dust emissions (Neff et al., 2008). When these crusts are disturbed, the soil loses its ability to resist wind-driven erosion and can blow away as dust. This removes nutrients from the soil and deposits them elsewhere (Belnap and Gillette, 1997; Neff et al., 2008). Further, when dust is deposited on winter snow cover, it can change the radiative forcing properties of the snow by reducing albedo. This effect can lead to more rapid and earlier snowmelt with significant impacts on runoff timing and quantity (Painter et al., 2007, 2010). These effects of dust on snow are important in Utah because the Wasatch Front metropolitan area of northern Utah, home to two million people and growing, relies heavily on snowmelt from the Wasatch Mountains for its water supply. Snowmelt contributes to surface and groundwater, and changes to the snow cover can affect these reservoirs.

In Utah, dust deposition rates have dramatically increased since the mid-19th century, likely due to increased grazing agriculture, and other human activities (Miller et al., 2012; Neff et al., 2008; Reynolds et al., 2010). Dust sources include playa surface deposits of Lake Bonneville such as Sevier Dry Lake, Tule Dry Lake, the Great Salt Lake Desert, the Milford Flat fire scar and metalliferous urban and industrial areas (Hahnenberger and Nicoll, 2012; Oviatt, 1997; Reynolds et al., 2013; Steenburgh et al., 2012).

Strontium (Sr) isotopes can be used to characterize dust provenance and movement through soils into vegetation. Strontium can be used as a tracer if the $^{87}Sr/^{86}Sr$ ratio varies in the sources and sinks under investigation. Strontium in soils and trees derives from weathering of parent material and atmospheric deposition. Deposited dust can contribute Sr to the soil by dissolution of the carbonate and labile (soil–water exchangeable) fraction and weathering of the silicate phases. Bulk soil, soil water, and secondary soil minerals maintain the Sr isotopic composition of the source material, although the isotopic ratio can be modified by mineral weathering and atmospheric deposition (Capo et al., 1998). While additional sources and processes can be involved in soil formation, such as climate, biological factors and recycling of organic matter, as a first approximation, soil formation may be considered a

* Corresponding author. Tel.: +1 503 701 3985.
E-mail addresses: olivia.miller@utah.edu (O.L. Miller), kip.solomon@utah.edu (D.K. Solomon), diego.fernandez@utah.edu (D.P. Fernandez), thure.cerling@utah.edu (T.E. Cerling), david.bowling@utah.edu (D.R. Bowling).

http://dx.doi.org/10.1016/j.apgeochem.2014.08.004
0883-2927/

two-component mixing process between atmospheric deposition and bedrock weathering (Lawrence et al., 2011; Graustein and Armstrong, 1983; Gosz et al., 1983; Capo et al., 1998, Stewart et al., 1998).

Strontium isotopes have been used to quantify natural and anthropogenic atmospheric inputs to ecosystems (Chiquet et al., 1999; Faure, 1977; Gosz et al., 1983; Grousset and Biscaye, 2005; Neff et al., 2008). Eghbal (1993), Rabenhorst (1984), and West (1988) found that parent rock was the most significant source of carbonates (and thus calcium and strontium) in soils they studied. Other researchers have found that dust was the most significant source in other locations (Capo and Chadwick, 1999; Chiquet et al., 1999; Dart et al., 2004; Stewart et al., 1998; Van der Hoven and Quade, 2002). Lawrence et al. (2011) used Sr and Nd isotopic mixing models to quantify dust accretion in San Juan Mountain soils. Åberg (1995) summarized many of the uses of Sr isotope ratios in detecting trends in soil and vegetation systems, including tree rings. Graustein and Armstrong (1983) used Sr isotopes to estimate that over 75% of the strontium in vegetation in the Sangre de Christo Mountains of New Mexico was atmospherically derived. English et al. (2001) measured $^{87}Sr/^{86}Sr$ in trees growing on different substrates (Precambrian granite, Paleozoic limestone and sandstone, Tertiary sandstone and basalt, and Pliocene basalt, and andesite) and found very little difference in the tree $^{87}Sr/^{86}Sr$ ratios within one mountain range but much greater differences between mountain ranges, which they attribute to the overriding influence of local and regional atmospheric dust sources of strontium.

Trees can be used as temporal monitors of environmental change because trees create annual growth rings. Dendroanalysis has long used measurements of trace elements in tree ring as records of pollution (Barnes, 1976; Beramendi-Orosco et al., 2013; Padilla and Anderson, 2002 and references within). Dendroanalysis assumes that the element concentrations within tree rings represent element availability in the trees environment (Padilla and Anderson, 2002). A variety of site-specific factors control element uptake by vegetation including the sapwood–heartwood concentration equilibrium, the quantity of macronutrients versus metals, ion solubility, soil type, and pH (Cutter and Guyette, 1993; Gerloff et al., 1966; Padilla and Anderson, 2002). Root uptake selectivity is also important (Bowen and Dymond, 1956; Roca and Vallejo, 1995). Via the roots, vegetation takes up Sr and nutrients from both the soil solution (water and ions held within soil by capillary action) and the soil exchange complex (the reservoir of ions attracted to negatively charged surfaces of organic matter and soil minerals) (Capo et al., 1998).

Strontium isotopes in tree rings have been proven to record chemical changes in soils (Drouet et al., 2005). In Sweden, changes in strontium isotopes in tree rings have been attributed to changes in the calcium content of soils (Åberg et al., 1990). Poszwa et al. (2003) modeled Sr isotope ratio changes in tree rings over time due to soil acidification, confirming that Sr isotopes in tree rings record the chemical history of the soil. While Åberg et al. (1990) and Poszwa et al. (2003) attribute the changes in Ca content of soils and Sr isotopes in tree rings over time to soil acidification, atmospheric deposition of dust could alter soil as well, particularly given the relatively high dust flux in the Wasatch Mountains ($\sim$400 g m^{-2} annually) (Steenburgh et al., 2012).

A record of dust deposition and sources is needed to put current sources of dust to the Wasatch Mountains into historical context. Such a record could indicate whether or not new dust sources have been created and how source activation changes over time. A record of dust sources and deposition would strengthen our understanding of the connections between human activities in dust source areas and their effect on dust formation. A record would also inform our understanding of the influence dust has on snow hydrology. We investigated whether Sr isotopes in tree rings can provide such a record. We have broadly identified variations in dust deposited on the Wasatch Mountains and quantified dust Sr contributions to soil and vegetation. The Sr contribution of dust was compared to the Sr contribution of three kinds of bedrock (granodiorite, quartzite, and limestone), which were estimated to have different Sr concentrations and isotopic ratios, and overlying soils and trees. This provided information about the relative contributions of dust and different bedrocks to Sr in soil and vegetation. From this analysis, we identified dust as a major source of Sr for soils and trees and demonstrated that trees record the Sr isotopic signal of dust in the Wasatch Mountains. Thus, the Sr isotopic record found in tree rings can be used to understand sources of dust deposition back in time.

2. Methods

2.1. Site description

The Wasatch Mountains run roughly 800 km north to south through northern Utah, forming the western edge of the Rocky Mountains at this latitude and the eastern (downwind) edge of the Basin and Range Province. Salt Lake City lies to the west at an elevation of *ca.* 1300 m, and the central Wasatch Mountains rise abruptly from the valley floor to a peak elevation of over 3400 m (Fig. 1). Slopes at the Little Cottonwood Canyon site (where bedrock, soil, and tree core samples were taken) are steep, and soils are poorly developed. Samples were taken on ridges with minimal influence of groundwater or soil or rock transported from higher elevations.

2.2. Dust event and meteorological observation

Dust events over the winter of 2011–2012 were observed and identification of the dust source was attempted using MODIS imagery, HYSPLIT modeling (Hybrid Single Particle Lagrangian Integrated Trajectory Model), meteorological data, and the authors' personal observation notes. MODIS images from the Railroad Valley Subset of AERONET were used to identify dust plume sources (NASA/GSFC/Earth Science Data and Information System). HYSPLIT modeling (Draxler and Rolph, 2012) was used to confirm dust source locations identified from MODIS images. Dust observations with meteorological data were obtained from the National Climate Data Center (NCDC, Salt Lake City International Airport station, hourly observations).

2.3. Sample collection

Dust samples were collected from three sites: Mill Creek Canyon (MCC), Big Cottonwood Canyon (BCC), and Little Cottonwood Canyon (LCC) (Fig. 1). Dust sample sites were located in clearings away from vegetation, had minimal impact from recreationists, avalanches, or roads. Dust from visible layers representing individual deposition events in the snow cover was collected to characterize the concentration and $^{87}Sr/^{86}Sr$ ratio of dust inputs to the Wasatch Mountains (Table 1). Collection on snow prevented contamination from the soil and allowed for isolation of individual dust events.

At each site a snow pit was excavated to obtain information on snow depth, layering, and dust layer depths. Snow above the dust layer was removed and dusty snow was scraped up in LDPE (low density polyethylene) wide-mouth 500 mL or 1000 mL plastic bottles. Field blanks were taken by leaving a bottle open for the time necessary to collect samples. Samples were kept frozen until analysis. Samplers wore new powder-free vinyl gloves and non-fibrous clothing to reduce contamination of samples. All plastic-ware used

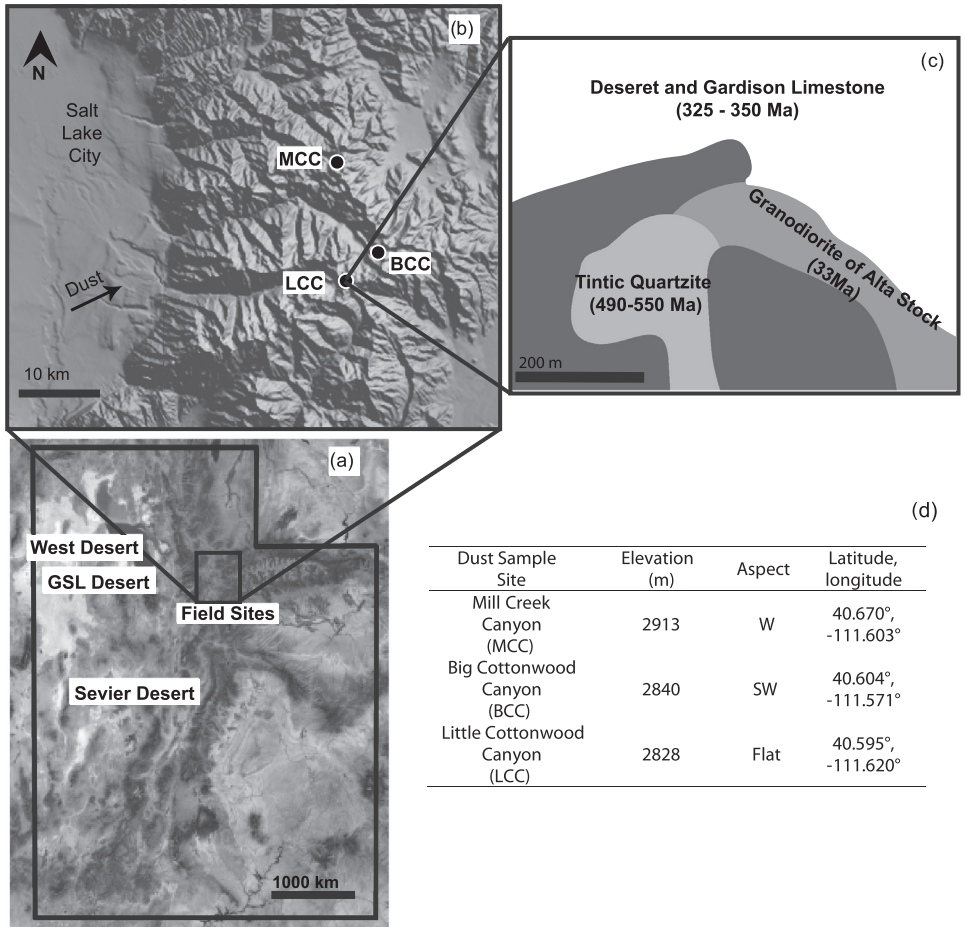

(d)

Dust Sample Site	Elevation (m)	Aspect	Latitude, longitude
Mill Creek Canyon (MCC)	2913	W	40.670°, -111.603°
Big Cottonwood Canyon (BCC)	2840	SW	40.604°, -111.571°
Little Cottonwood Canyon (LCC)	2828	Flat	40.595°, -111.620°

Fig. 1. Map and description of sample sites. (a) Dust sources identified in this study and field site locations. (b) All field sampling sites. (c) Bedrock, soil, and tree sampling site in LCC. (d) Dust sampling site descriptions. Dust was collected at all three sites (MCC, BCC, LCC). Bedrock samples of Alta Stock Granodiorite, Deseret and Gardison Limestone (undifferentiated), and Tintic Quartzite were collected at Little Cottonwood Canyon site, as well as two cores from ten trees over each bedrock type, and soil samples from below every tree. Geologic map adapted from (James et al., 1978). Source areas show sources identified in this study. See Steenburgh et al. (2012) for additional dust sources.

Table 1
Dust events, deposition dates, sampling dates, and source areas identified. Dust from events 5,6, and 7 was not observed at all sites and were not included in chemical analysis.

Dust event	Deposition date	MCC sample date	BCC sample date	LCC sample date	Source areas
1	12/31/2011	3/24/2012	1/14/2012	3/10/2012	Unknown
2	2/23/2012	3/24/2012	3/3/2012	3/10/2012	GSL Desert
3	2/25/2012	3/24/2012	3/3/2012	3/10/2012	GSL Desert
4	3/6/2012	3/24/2012	3/24/2012	3/10/2012	Unknown
5	3/17/2012	3/24/2012	3/24/2012	No dust	Unknown
6	Unknown	3/24/2012	No dust	No dust	Unknown
7	3/19 or 3/20/2012	3/24/2012	No dust	No dust	Unknown
8	3/31/2012	4/6/2012	4/7/2012	4/7/2012	West Desert, Sevier Desert

for snow sampling and analysis was acid-washed and dried in a laminar flow bench prior to use.

Bedrock samples were collected from below each tree cored as float (loose pieces of rock not connected to an outcrop). Bedrock formations sampled include the Granodiorite of the Alta Stock (Oligocene, 33 Ma), the Deseret and Gardison limestone (undivided, Upper and Lower Mississippian, ~325–355 Ma), and the Tintic Quartzite (Middle and Lower Cambrian, ~490–550 Ma) (Bryant, 1990; James et al., 1978). The different rock types were hypothesized to have different Sr isotope concentrations and ratios, which, along with dust, would serve as endmembers to compare soils and trees to. The granodiorite of the Alta Stock was predicted to have a low Sr concentration and distinct Sr isotope ratio between 0.707 and 0.708 (Vogel et al., 2001) because of the high potassium feldspar content of the igneous rock. Within potassium feldspar rich rocks, rubidium (Rb) can substitute for potassium (K), and ^{87}Rb decays radioactively to ^{87}Sr. Over time, more ^{87}Sr is produced, while the ^{86}Sr remains constant, thus producing a higher ^{87}Sr/^{86}Sr ratio. The Deseret and Gardison Limestone was predicted to have a very high Sr concentration, which could increase the Sr concentration in soils and trees overlying the bedrock, because of the high concentration of Ca in limestone and substitution of Sr for Ca. The limestone was also estimated to have an ^{87}Sr/^{86}Sr ratio close to 0.707 (Capo et al., 1998). The Tintic Quartzite, composed almost completely of quartz was expected to have very little Sr, allowing this site to serve as a test of total dust influence for Sr input (Lindgren et al., 1919). These estimates of Sr concentration and ^{87}Sr/^{86}Sr ratio were simply used for experimental design, and rock

samples of each type were analyzed for later calculations of dust and bedrock contribution to soil and tree Sr. The sampling strategy enabled us to evaluate differences in bedrock contribution of Sr to soil and vegetation.

Soil samples were taken from below each tree cored. Soil samples were taken from 10 cm depth, 1 m from the tree, on the south side of the tree. Some variability existed within sample location specifics due to thin soils, and vegetation and outcrop presence.

Tree cores were taken from Engelmann spruce, *Picea engelmannii*, growing on the three different bedrock types sampled. Trees were within 500 m of each other at the Little Cottonwood Canyon site. This ensured that the trees were all receiving similar dust Sr input but different bedrock Sr input. Two cores were taken from the south side of each tree (ten trees/bedrock type, thirty trees total) using a 5.15 mm diameter increment borer to characterize natural heterogeneity within each tree and between all trees. Several trees had to be cored on a more easterly side of the tree due to the presence of branches or site topography. Root depths varied. Rooting depths of Engelmann spruce growing in shallow soils over impervious rocks can be up to 46 cm, although Engelmann spruce growing in deep soils can be over 2.4 m (Alexander and Shepperd, 2004). However, many trees sampled for this study had exposed roots and roots growing directly on rock and within rock cracks. Cores were transported in plastic straws back to the laboratory for drying and analysis.

2.4. Sample preparation

Snow containing dust was melted, filtered with a 0.5 mm mesh to remove large organic matter such as pine needles, centrifuged and allowed to settle overnight before excess water was decanted. Dust was allowed to dry in a laminar flow hood for five days, after which it was digested using the cold leach method (Carling et al., 2012), in preparation for Sr concentration and $^{87}Sr/^{86}Sr$ analysis. The cold leach involved leaching dust in between 2–10 mL (depending on the mass of dust) 0.8 M HNO_3 (5%v/v) at 22 °C for 24 h. Volume of HNO_3 varied to achieve an estimated 1:500 dilution, based on the mass of dust in each sample. This leach method is a partial digestion meant to dissolve more environmentally accessible Sr including the exchangeable, carbonate-bound, and organic fractions (Lawrence et al., 2010). Dust grains insoluble in 4 M HNO_3 acid were not included in this analysis as we were trying to evaluate the bioavailable Sr.

Lawrence et al. (2010) used a sequential leach of 1 M ammonium acetate, 1 M acetic acid, and 1 M HNO_3 to target exchangeable, carbonate-bound, and organic fractions. These treatments target more environmentally available elements. Vegetation generally sources base cations from the exchangeable reservoir (Stewart et al., 1998). Thus, the 4 M HNO_3 treatment targets those same fractions, and partially addresses that alteration process over time, without introducing elements bound in minerals that would "not be expected to be released in solution over a reasonable time span under the conditions normally encountered in nature" (the residual fraction of Tessier (1979)). Further, a total digestion was not applied as elements bound in silicate structures (residual fraction) are not commonly mobile in the environment (USEPA, 1996). Within the soil, the most bioavailable and mobile substances are those that are water soluble, exchangeable, or weak acid soluble (Baruah et al., 2011). The $^{87}Sr/^{86}Sr$ values obtained using the cold leach method on the dust are expected to be similar to those obtained using acetic acid for the bedrock, and soil collected in this study. The effect of cold leach and a milder leaching method (pH = 4.5 ammonium acetate buffer) were compared for two Av horizon soils developed on rhyolite and quartzite bedrocks in the Sevier Desert area. For both soils the Sr extracted with the buffer was >99% of the Sr extracted with the cold leach method, and the corresponding $^{87}Sr/^{86}Sr$ values agreed within 0.00005. These soils contained ~10% (by weight) carbonate, comparable to the dust collected in this study. The cold leach method was selected to allow for comparison with soil samples taken from potential dust sources that had been previously analyzed using this leach method (S. Hynek, personal communication, January 28, 2012).

Snowmelt (30 mL) was decanted from each sample and preserved with 1 M HNO_3. There was a much larger volume of snowmelt than dust and only a small volume of snowmelt was decanted relative to the total volume of snowmelt. While it is possible that some very small fraction of the particulate matter was included in the snowmelt analysis, it would be a very small amount. It is also possible that some of the highly soluble minerals dissolved in the snowmelt. However, the mixing calculations treat the acid and water soluble fractions together, and so a small amount of particulate matter in the decanted snowmelt would not change our conclusions. The total dust signal analyzed includes both the water-soluble fraction (snowmelt) and acid-soluble fractions. The term "total dust" refers to combined snowmelt and dust fractions, unless otherwise indicated.

Two soil samples from each bedrock type were sieved to 0.5 mm to remove large pieces of rock and organic material. After soils were allowed to dry, 20 mL of 1 M acetic acid was added to 1 g of soil and allowed to leach for 24 h on a shaker table to remove carbonates. Samples were then centrifuged, and 5 mL of primary leachate was removed and evaporated to remove the acetic acid. Dried leachate was acidified with 5 mL clean 5% HNO_3 (samples must be in HNO_3 for inlet into mass spectrometer).

Two quartzite and two granodiorite rock samples were cut to remove the outer weathered rinds and expose only pristine rock. Chips of these unweathered samples were powdered with an agate mortar and pestle before undergoing the same leach process described in the soil analysis section.

Tree cores were dried before being sanded and rings counted and matched across cores. Skeleton plots were constructed to aid in ring matching (Stokes, 1996). Strontium concentration and $^{87}Sr/^{86}Sr$ ratio was measured in sections of tree core composed of rings formed between 1983 and 1987 (five rings/core) from all trees sampled. These years were selected because rings produced over these years were easily identifiable across all cores. This allowed for comparison of the same five rings from every core. To identify temporal changes within one core, all rings were analyzed in groups of five consecutive rings. The rings were analyzed in groups of five in order to ensure sufficient Sr abundance for concentration and isotopic measurement.

Tree rings were cleaned in an ultrasonic bath to remove contamination from sanding and dried prior to microwave digestion using 2.5 mL ultrapure concentrated HNO_3 (16 M) and 0.625 mL hydrogen peroxide (30%). The microwave digestion program involved four stages, all at up to 1000 Watts: (1) 2 min increasing temperature to 85 °C, (2) 5 min increasing temperature to 145 °C, (3) 3 min increasing temperature to 200 °C, and (4) 20 min at 200 °C. Digests were diluted to 1:100 prior to elemental analysis.

For isotopic measurement, digests were evaporated on a hot plate to concentrate Sr and to remove concentrated HNO_3 and hydrogen peroxide so that samples could be introduced into the mass spectrometer, which requires an inlet HNO_3 concentration of 4 M HNO_3. Immediately prior to sample inlet, dried samples were re-acidified with 2.67 mL 4 M HNO_3.

2.5. Sample analysis

Elemental concentrations of all samples were measured using inductively coupled plasma quadrupole-mass spectrometry on an Agilent 7500ce instrument (Agilent Technologies, Santa Clara, California, USA). Indium (5 ppm) was used as an internal standard

for elemental analysis. Strontium isotope ratios of all samples were measured via multi-collector inductively coupled plasma mass spectrometry using a Thermo Scientific Neptune (Bremen, Germany). Strontium isotopic measurements were run using the SrFast method (Mackey and Fernandez, 2011). Briefly, 4 M HNO_3 sample fractions (dust or soil leachates; tree-rings digests) containing 40–80 ng of Sr were automatically purified using a column containing Eichrom Sr-resin (Lisle Illinois) and introduced in the mass-spectrometer using a system containing two 6-way valves and an autosampler (Elemental Scientific, Omaha, NE). NIST SRM 987 $SrCO_3$ isotopic standard fractions containing 80 ng of Sr were run (using the same purifying system) every three samples. Blanks were run between every sample and standard and a correction to samples and isotopic standards was performed using the previous blank run. Long-term $^{87}Sr/^{86}Sr$ value for the isotopic standard using this method is 0.71030 ± 0.00002 ($N > 1000$, 2σ).

3. Results

3.1. Dust event meteorology

For the Wasatch Mountains, the 2011–2012 winter was characterized by very dry conditions, which contributed to drought throughout the summer and fall. Eight dust events, defined by their creation of a visible dust layer in the snow cover, were observed over the period from December 2011 to March 2012 (Table 1). However, only five events had enough dust volume to analyze at all three sites (D1, D2, D3, D4, and D8) (Table 1). Sample analysis for some events (D5, D6) was possible for some sites. D7 was omitted from further study due to low sample mass at all sites. Due to low snow abundances, dust events after D8 were unusable as there was no snow in between dust events to isolate dust layers. This led to the omission of several dust events during the main dust season of March through May (Steenburgh et al., 2012).

Observed dust sources include the Great Salt Lake Desert (GSL Desert), the West Desert, the Sevier Desert. However, sources of two events (D1, D4) were unidentifiable using MODIS images. On days when dust events occurred, wind speeds at the Salt Lake City International Airport ranged from 3 to 40 mph, with gusts between 21 and 59 mph. When dust event timing could be determined, dust events tend to begin mid-day to early afternoon. Wind direction ranged from south to west to north (160–10 compass degrees).

3.2. Dust samples

Acid-soluble dust samples from the same event but different locations had similar $^{87}Sr/^{86}Sr$ ratios, although the Mill Creek site was the largest outlier for this pattern (Table 2). Samples of individual dust events tended to cluster together within a range of $^{87}Sr/^{86}Sr$ ratios of 0.71020–0.71236 (or 0.71165 when median absolute deviation, MAD, was used to remove outliers) and concentration range of 15–1573 μg/g (or 111 when MAD was used) (Fig. 2). These acid-soluble dust samples fell within the range of Sevier Desert soil samples that represent potential dust source areas (S. Hynek, personal communication, March 6, 2012).

Water-soluble dust samples (snowmelt) had similar Sr isotope ratios as acid-soluble dust samples, but different Sr concentrations (Table 3). The $^{87}Sr/^{86}Sr$ ratio in snowmelt and acid-soluble dust had a 1:1 relation, with a slope = 1.0, $r^2 = 0.83$. Although evidence was sparse or lacking for isotopic fractionation caused by or during melting of snow, such fractionation cannot be ruled out because of scatter in the data. Such fractionation would cause the snowmelt and acid-soluble dust to have different $^{87}Sr/^{86}Sr$ ratios. However, fractionation due to biological processes and phase changes such as dissolution or precipitation is too small to measure (Capo

Table 2
Strontium concentration and $^{87}Sr/^{86}Sr$ isotope ratio in acid-soluble (dust) fractions of dust. BCC = Big Cottonwood Canyon, LCC = Little Cottonwood Canyon, MC = Mill Creek Canyon. b indicates a duplicate sample was taken. The uncertainty of the Sr concentration in parenthesis is based on a standard uncertainty multiplied by a coverage factor $k = 2$, providing a level of confidence of approximately 95%. The error on the $^{87}Sr/^{86}Sr$ measurement is the standard error of multiple isotope ratio measurements.

Event	Sr (μg/g)	$^{87}Sr/^{86}Sr$
LCC 1	41.5 (0.2)	0.71037 (0.00002)
MCC 1	72.7 (0.1)	0.71033 (0.00001)
BCC 2	886 (8)	0.71157 (0.00003)
LCC 2	184.3 (0.1)	0.71180 (0.00001)
MCC 2	174.9 (0.2)	0.71082 (0.00001)
BCC 3	15.7 (0.4)	0.71083 (0.00003)
BCC 3b	236.4 (0.7)	0.71071 (0.00001)
LCC 3	96.0 (0.2)	0.71078 (0.00001)
MCC 3	1573 (9)	0.71121 (0.00001)
BCC 4	42.4 (0.2)	0.71036 (0.00001)
LCC 4	34.9 (0.2)	0.71061 (0.00002)
LCC 4b	57.7 (0.2	0.71064 (0.00001)
MCC 4	688.8 (0.1)	0.71236 (0.00001)
MCC 5	111.8 (0.2)	0.71165 (0.00001)
MC DL 6	53.8 (0.1)	0.71035 (0.00001)
LCC 8	37.2 (0.2)	0.71020 (0.00002)
MCC 8	45.5 (0.2)	0.71032 (0.00002)
MCC 8	75.6 (0.3)	0.71033 (0.00001)

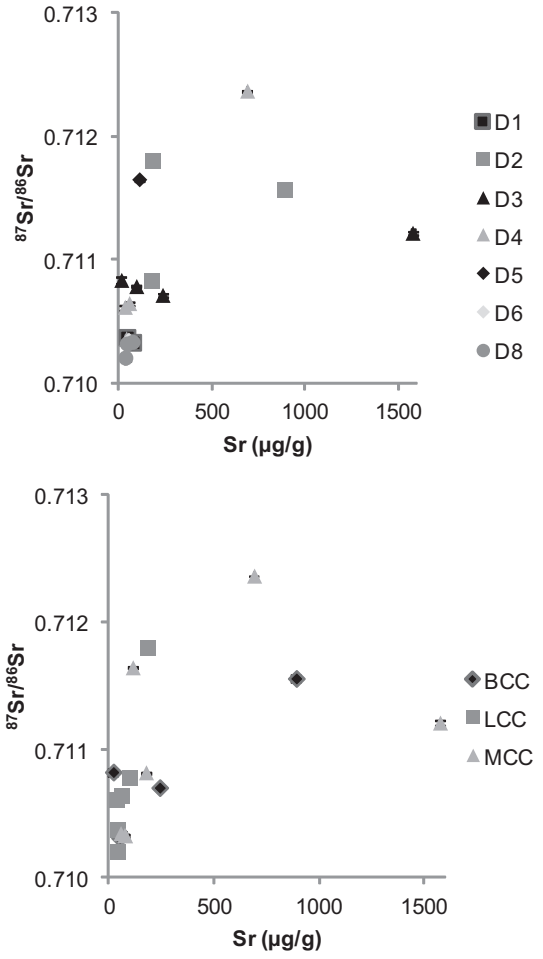

Fig. 2. $^{87}Sr/^{86}Sr$ ratio versus Sr concentration of acid-soluble dust samples. (a) Different dust deposition events, corresponding to dates in Table 1. (b) Different sites where BCC = Big Cottonwood Canyon, LCC = Little Cottonwood Canyon, and MCC = Mill Creek Canyon.

Table 3
Strontium concentration and $^{87}Sr/^{86}Sr$ isotope ratio in water-soluble (snowmelt) fractions of dust. Snowmelt Sr concentration has been normalized to mass of dust. BCC = Big Cottonwood Canyon, LCC = Little Cottonwood Canyon, MC = Mill Creek Canyon. b indicates a duplicate sample was taken. The uncertainty of the Sr concentration is based on a standard uncertainty multiplied by a coverage factor $k = 2$, providing a level of confidence of approximately 95%. The error on the $^{87}Sr/^{86}Sr$ measurement is the standard error of multiple isotope ratio measurements.

Event	Sr (μg/g)	$^{87}Sr/^{86}Sr$
LCC 1	1263 (17)	0.71052 (0.00003)
MC 1	795 (4)	0.71034 (0.00002)
BCC 2	227653 (6)	0.71195 (0.00002)
LCC 2	2736 (4)	0.71216 (0.00002)
MC 2	4540 (3)	0.71096 (0.00002)
BCC 3	4437 (7)	0.71132 (0.00002)
BCC 3b	15889 (7)	0.71148 (0.00002)
LCC 3	5540 (4)	0.71105 (0.00002)
MC 3	176437 (9)	0.71187 (0.00002)
BCC 4	492 (64)	0.71088 (0.00006)
LCC 4	641 (86)	0.71068 (0.00007)
LCC 4b	904 (58)	0.711 (0.00006)
MC 4	3599 (2)	0.71217 (0.00001)
MC 5	4976 (3)	0.71203 (0.00002)
MC 6	1276 (13)	0.71067 (0.00003)
BCC 8	350 (20)	0.7109 (0.00004)
LCC 8	269 (8)	0.71057 (0.00003)
MC 8	4435 (17)	0.71081 (0.00003)

et al., 1998; Van der Hoven and Quade, 2002). The Sr concentration of the water-soluble fraction, which has been normalized to mass of dust per liter of snow, was greater than the acid-soluble fraction. Ultimately the dust Sr signal available to vegetation includes the water and acid soluble fractions of dust.

3.3. Bedrock samples

The granodiorite and limestone rock samples had lower $^{87}Sr/^{86}Sr$ ratios than acid and water-soluble dust (average $^{87}Sr/^{86}Sr$ ratio of granodiorite was 0.70922 ± 0.00003 and limestone was 0.70994 ± 0.0004) while the quartzite rock samples had much higher ratios (average quartzite $^{87}Sr/^{86}Sr$ ratio was 0.72951 ± 0.008) (Table 4). Quartzite and granodiorite rock samples Sr concentrations were very similar, and low (average rock Sr concentration <3 μg/g). Limestone Sr concentrations were much higher (average was 172 ± 34 μg/g). Note that all measurements are an approximation of the Sr available to vegetation as the leaches used target environmentally available elements.

3.4. Soil samples

All soils had similar $^{87}Sr/^{86}Sr$ ratios (Table 5). Soil developed over quartzite was slightly more radiogenic, followed by soil developed over granodiorite, then soil developed over limestone

Table 4
Strontium concentration and $^{87}Sr/^{86}Sr$ ratio measurements of bedrock samples. G = granodiorite bedrock, L = limestone bedrock, Q = quartzite bedrock. Number corresponds to the tree under which the sample was taken. The uncertainty of the Sr concentration is based on a standard uncertainty multiplied by a coverage factor $k = 2$, providing a level of confidence of approximately 95%. The error on the $^{87}Sr/^{86}Sr$ measurement is the standard error of multiple isotope ratio measurements.

Rock	Sr (μg/g)	$^{87}Sr/^{86}Sr$
Q11 rock	2 (1)	0.73719 (0.00002)
Q1 rock	2 (1)	0.72182 (0.00002)
G2 rock	1 (2)	0.70919 (0.00002)
G6 rock	1 (2)	0.70925 (0.00002)
L1 rock	206.3 (0.2)	0.71036 (0.000009)
L3 rock	137.6 (0.3)	0.70951 (0.000009)

Table 5
Strontium concentration and $^{87}Sr/^{86}Sr$ ratio measurements of soil samples taken over different bedrock types. G = granodiorite bedrock, L = limestone bedrock, Q = quartzite bedrock. Number corresponds to the tree under which the sample was taken. The uncertainty of the Sr concentration is based on a standard uncertainty multiplied by a coverage factor $k = 2$, providing a level of confidence of approximately 95%. The error on the $^{87}Sr/^{86}Sr$ measurement is the standard error of multiple isotope ratio measurements.

Soil	Sr (μg/g)	$^{87}Sr/^{86}Sr$
Q11 soil	26.9 (0.2)	0.71127 (0.00002)
Q1 soil	20.1 (0.2)	0.71124 (0.00002)
G2 soil	15.5 (0.3)	0.71139 (0.00002)
G6 soil	17 (0.3)	0.71088 (0.00001)
L1 soil	28.3 (0.6)	0.71049 (0.00002)
L3 soil	70.2 (0.3)	0.71144 (0.00002)

(average quartzite soil = 0.71126 ± 0.00001, average granodiorite soil = 0.71113 ± 0.0003, average limestone soil = 0.71097 ± 0.0005). Soil samples, regardless of bedrock type they formed over, very strongly resembled acid and water-soluble dust in their Sr isotopic ratios. Soil developed on limestone had the most Sr (average = 49.3 ± 21 μg/g), followed by soil developed on quartzite (average = 23.5 ± 3 μg/g), and then soil developed on granodiorite (average = 16.3 ± 1 μg/g).

3.5. Tree ring samples

Tree ring Sr isotope ratios and concentrations are shown in Fig. 3 and Table 6. Strontium isotope ratios and concentrations varied by bedrock type. The average $^{87}Sr/^{86}Sr$ ratio for trees over quartzite, granodiorite, and limestone was 0.71173 ± 0.0001, 0.71084 ± 0.00008, and 0.70971 ± 0.0002. The average Sr concentration in trees over quartzite, granodiorite, and limestone was 5 ± 0.3 μg/g, 4 ± 0.2 μg/g, and 3 ± 0.2 μg/g.

Two cores from the same tree were compared with each other for both $^{87}Sr/^{86}Sr$ ratio and Sr concentration to understand some of the natural heterogeneity of the tree rings (Fig. 4). The geometric mean regression is useful when either variable could be the independent variable because it minimizes the vertical and horizontal residuals, not just the vertical residuals as occurs when using the

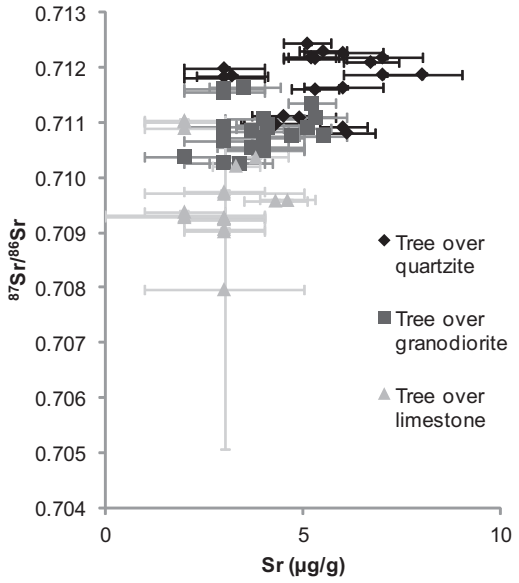

Fig. 3. Sr concentration versus $^{87}Sr/^{86}Sr$ isotope ratio in trees growing on different bedrock types.

Table 6
Strontium concentration and $^{87}Sr/^{86}Sr$ ratio measurements of the same consecutive five rings from trees growing over different bedrock types. G = granodiorite bedrock, L = limestone bedrock, Q = quartzite bedrock. Number indicates the tree number for each bedrock type. A and B signify the two cores taken from each tree. X indicates a duplicate was taken. For G6, cores were taken from four sides of the tree as indicated by the cardinal direction. The uncertainty of the Sr concentration is based on a standard uncertainty multiplied by a coverage factor $k = 2$, providing a level of confidence of approximately 95%. The error on the $^{87}Sr/^{86}Sr$ measurement is the standard error of multiple isotope ratio measurements.

Tree core	Sr (μg/g)	$^{87}Sr/^{86}Sr$
G1A	3 (1)	0.71154 (0.00002)
G1B	5.2 (0.6)	0.71135 (0.00001)
G2A	3.5 (0.9)	0.71164 (0.00002)
G2B	3 (1)	0.71161 (0.00002)
G3A	4.1 (0.8)	0.71096 (0.00001)
G3B	4.1 (0.8)	0.71091 (0.00001)
G4A	4 (1)	0.71056 (0.00002)
G4B	4 (1)	0.71053 (0.00002)
G5A	3 (1)	0.71067 (0.00002)
G5B	4 (1)	0.71073 (0.00002)
G6 East	3.7 (0.9)	0.71054 (0.00021)
G6 North	3 (1)	0.71027 (0.00002)
G6 West	3 (1)	0.71092 (0.00002)
G6A South	2 (1)	0.71038 (0.00002)
G6B South	3.4 (0.8)	0.71025 (0.00001)
G7A	4 (1)	0.71052 (0.00002)
G7B	4 (1)	0.71049 (0.00002)
G8A	4.7 (0.7)	0.71076 (0.00001)
G8B	5.5 (0.6)	0.71076 (0.00002)
G9A	5.1 (0.6)	0.7109 (0.00001)
G9B	3.7 (0.9)	0.71085 (0.00002)
G10A	5.3 (0.8)	0.71108 (0.00001)
G10B	4 (1)	0.71107 (0.00002)
L1A	3 (1)	0.70927 (0.00002)
L1B	3 (1)	0.70924 (0.00002)
L2A	2 (1)	0.70938 (0.00002)
L2B	3 (1)	0.70974 (0.00002)
L3A	2 (1)	0.71104 (0.00002)
L3B	2 (1)	0.71102 (0.00002)
L4A	2 (1)	0.71102 (0.00002)
L4B	2 (1)	0.7109 (0.00002)
L5A	3 (1)	0.70927 (0.00002)
L5B	3 (1)	0.70926 (0.00002)
L6A	2 (2)	0.70931 (0.00002)
L6B	2 (2)	0.70928 (0.00002)
L7A	3 (1)	0.70906 (0.00001)
L7B	3 (1)	0.70902 (0.00002)
L8A	4.3 (0.8)	0.70958 (0.00001)
L8B	4.6 (0.7)	0.70959 (0.00001)
L9A	3.8 (0.8)	0.71036 (0.00001)
L9B	3.3 (0.6)	0.71021 (0.00001)
L10A	3 (2)	0.70797 (0.0029)
L10B	3 (2)	0.7097 (0.00002)
Q1A	5.2 (0.7)	0.71218 (0.00001)
Q1B	5.2 (0.6)	0.71218 (0.00001)
Q2A	3 (1)	0.71198 (0.00002)
Q2AX	6.7 (0.7)	0.71209 (0.00001)
Q2B	5.1 (0.6)	0.71243 (0.00001)
Q3A	6 (1)	0.71226 (0.00002)
Q3B	7 (1)	0.71218 (0.00002)
Q4A	3 (1)	0.71182 (0.00002)
Q4B	3.2 (0.9)	0.71185 (0.00002)
Q5A	5.3 (0.8)	0.71216 (0.00001)
Q5B	5.5 (0.6)	0.71229 (0.00001)
Q6A	6 (1)	0.71163 (0.00002)
Q6B	5.3 (0.6)	0.7116 (0.00001)
Q7A	4.9 (0.9)	0.71109 (0.00002)
Q7B	4.5 (0.8)	0.71111 (0.00001)
Q8A	4.2 (0.8)	0.71098 (0.00001)
Q8B	4.3 (0.8)	0.71097 (0.00001)
Q9A	6.1 (0.7)	0.71081 (0.00001)
Q9B	6 (0.6)	0.71091 (0.00001)
Q11A	7 (1)	0.71187 (0.00002)
Q11B	8 (1)	0.71187 (0.00002)

ordinary least squares regression (Ricker, 1973; Zobitz et al., 2006). Tree rings from the same five years taken from two cores from the same trees matched very well for $^{87}Sr/^{86}Sr$ ratio and moderately well for Sr concentration as described below.

The isotope ratios for two cores from the same tree are close to agreement. The GMR slope ranged from 0.94 to 1.05 and the r^2 ranged from 0.92 to 0.96. For trees growing on quartzite, the GMR slope was 1.05 and the r^2 was 0.93. For trees growing on granodiorite, the GMR slope was 0.97 and the r^2 value was 0.97. For trees growing on limestone, the GMR slope was 0.94 and the r^2 was 0.96. There was a very close relationship between the $^{87}Sr/^{86}Sr$ ratios in two cores taken from the same tree for all trees, regardless of bedrock type (GMR slope = 1.01, $r^2 = 0.97$).

The Sr concentration in two cores from the same tree was close, although some bedrock dependent variability existed. For trees growing on quartzite, the GMR slope was 1.02 and the r^2 was 0.67. For trees growing on granodiorite, the GMR slope was 0.73 and the r^2 value was 0.03. For trees growing on limestone, the GMR slope was 0.96 and the r^2 was 0.78. The variability of Sr concentration in trees growing over granodiorite is greater than the variability in trees growing over quartzite or limestone. When all trees were considered without regard for bedrock type, the GMR slope was 1.01, $r^2 = 0.68$. Two cores from the same tree growing on limestone and quartzite have a nearly 1:1 relationship between the Sr concentrations, while two cores from the same tree growing on granodiorite have a weaker relationship. Disregarding bedrock type, natural heterogeneity existed in Sr concentration, although it was not very strong.

One tree was cored on the north, west, and east side, in addition to the two cores taken on the south side (five cores total from one tree) to characterize directional variation of Sr isotopes and concentration. Little variation existed among cores taken on different sides of the same tree. The average and standard deviation of $^{87}Sr/^{86}Sr$ ratios for cores taken from four sides of the same tree was 0.71047 and 0.0002, whereas the average and standard deviation of the concentration was 3 μg/g and 0.6 μg/g. The largest range in isotopic ratios was between the core taken on the west side of the tree and a core taken on the south side of the tree (G6 West = 0.71092, G6B South = 0.71025). The largest range in Sr concentration was between the core taken on the east side of the tree and one core taken on the south side (G6 East = 3.7 μg/g, G6A South = 2.0 μg/g).

3.6. Sources of strontium for trees

Dust is a major source of Sr to trees (Fig. 5). Strontium isotopic ratios and concentrations suggested that trees growing on quartzite and granodiorite obtained much of their Sr from dust and trees growing on limestone obtained some of their Sr from dust and some from the weathered bedrock. Tree samples, particularly from trees growing over quartzite or granodiorite, have $^{87}Sr/^{86}Sr$ that are closer to the $^{87}Sr/^{86}Sr$ of dust than the underlying bedrock.

Despite the strong dust influence, some bedrock influence on tree rings was measured, mostly for trees growing over limestone. Some tree ring samples fell outside of the range of the total dust Sr ratio standard error of the mean, meaning they were significantly different than dust and that bedrock partially influenced their $^{87}Sr/^{86}Sr$ ratios. $^{87}Sr/^{86}Sr$ ratios of trees growing over quartzite and granodiorite were more similar to dust $^{87}Sr/^{86}Sr$ ratios than $^{87}Sr/^{86}Sr$ ratios of trees growing over limestone, suggesting that the trees growing over quartzite and granodiorite sourced more Sr from dust than did trees growing over limestone. Even though the samples were not identical to dust, they were more similar

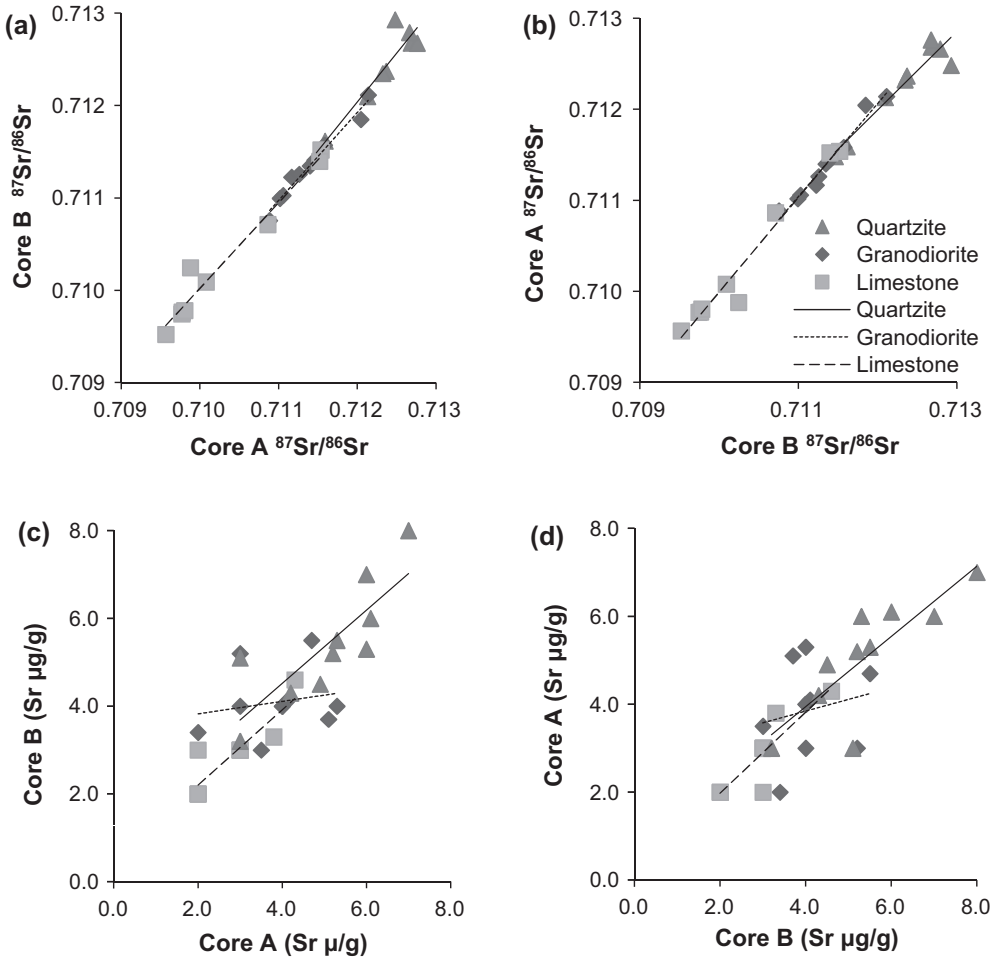

(e)

Bedrock	Independent Variable	$^{87}Sr/^{86}Sr$ ratio		Sr concentration	
		Slope	y-intercept	Slope	y-intercept
Quartzite	Core A	1.02	-0.01	0.84	1.18
	Core B	0.91	0.06	0.8	0.75
Granodiorite	Core A	0.95	0.03	0.14	3.54
	Core B	1.02	-0.02	0.27	2.78
Limestone	Core A	0.92	0.05	0.86	0.48
	Core B	1.04	-0.02	0.92	0.13

Fig. 4. Plots comparing the $^{87}Sr/^{86}Sr$ ratio and Sr concentration in two cores (A and B) from each tree. (a) Core A $^{87}Sr/^{86}Sr$ versus Core B $^{87}Sr/^{86}Sr$. (b) Core B $^{87}Sr/^{86}Sr$ versus Core A $^{87}Sr/^{86}Sr$. (c) Core A Sr concentration versus Core B Sr concentration. (d) Core B Sr concentration versus Core A Sr concentration. (e) Slope and *y*-intercept of regressions using both independent variables (Core A and Core B) that were used to calculate GMR and r^2.

to dust than to the bedrock they grow over, suggesting that the main source of Sr was dust.

3.7. Mixing models

Mixing models were used to understand the role of various Sr sources to soil and tree rings. End member components included dust and bedrock while mixtures included soil and trees. Total dust Sr is composed of the water soluble (snowmelt), acid soluble (dust leach), and insoluble (dust grains) fractions. For this analysis the water and acid soluble fractions were combined to calculate the total dust end member of the mixing model because they are the only fractions available to vegetation. Analysis of dust, bedrocks, soils, and trees suggested that dust was a very important source of Sr in this system.

Dust contribution to soil and tree Sr was calculated. For a mixture of two end members, the fraction of Sr from one component is given by:

$$\frac{M_1^{Sr}}{M_1^{Sr}+M_2^{Sr}}=\frac{R_m-R_2}{R_1-R_2} \quad (1)$$

where $R = {}^{87}Sr/^{86}Sr$, M_n^{Sr} = the mass of Sr in component n, and m denotes the mixture (Stewart et al., 1998). From this calculation, 94–100% of the Sr in soils over quartzite was from dust, 63–100% of the Sr in soils over granodiorite was from dust, and 50–100% of Sr in soils over limestone was from dust. The range of percentages was calculated using the average, average plus standard error, and average minus standard error of the $^{87}Sr/^{86}Sr$ ratios of total dust, bedrock, and soil measurements. Extending this to trees, 85–100%

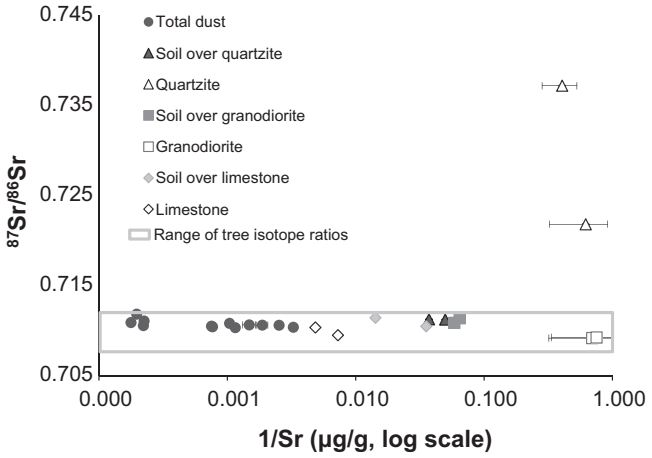

Fig. 5. Cross plot of $^{87}Sr/^{86}Sr$ ratios and 1/Sr concentrations on log scale for all dust, bedrock, and soil samples measured. Gray box indicates range of tree $^{87}Sr/^{86}Sr$. $^{87}Sr/^{86}Sr$ measurement standard error bars are smaller than symbol size (max ± 0.00007). Concentration uncertainty indicated by error bars.

of the Sr in trees growing over quartzite was from dust, 55–100% of Sr in trees growing over granodiorite was from dust, and 0–92% of Sr in trees growing over limestone was from dust. There is no observed association between soil depth and Sr source for the trees growing over limestone that sourced more of their Sr from dust. These calculations clearly indicate that dust was the major contributor of Sr to soil and trees.

The proportion of dust to soil was also calculated using the following equation

$$\frac{M_1}{M_1+M_2}=\frac{Sr_2(R_m-R_2)}{Sr_2(R_m-R_2)+Sr_1(R_1-R_m)} \quad (2)$$

where $R = {}^{87}Sr/^{86}Sr$, M_n = the mass of component n, and Sr_n = Sr concentration of component n, and m denotes the mixture (Stewart et al., 1998). Eq. (2) indicated that the contribution of dust to bioavailable soil composition is between 93% and 100% of bioavailable soil developed on quartzite. Between 95% and 100% of soil over granodiorite was dust and between 0% and 48% of soil over limestone was dust. For these calculations, the average, average plus standard error, and average minus standard error, of total dust, soil, tree, and bedrock values were used.

To calculate the $^{87}Sr/^{86}Sr$ ratio of a mixture, the following equation can be used (Faure, 1977):

$$R_m=\frac{Sr_1Sr_2(R_2-R_1)}{Sr_m(Sr_1-Sr_2)}+\frac{Sr_1R_1-Sr_2R_2}{Sr_1-Sr_2} \quad (3)$$

where $R_n = {}^{87}Sr/^{86}Sr$ of component n and Sr_n = Sr concentration of component n. The robustness of this mixing model was tested to evaluate how appropriate the application of a simple two-component mixing model is for understanding Sr movement through soils and trees.

This mixing model worked well when considering soils as a mixture of bedrock and dust. For soils formed over quartzite, the model predicted an average $^{87}Sr/^{86}Sr$ ratio of 0.71261, while the measured average value was 0.71126 (a difference of .001). For soils formed over granodiorite, the model predicted an average $^{87}Sr/^{86}Sr$ ratio of 0.71087, while the measured average value was 0.71086 (a difference of 0.00001). Average soil, average total dust, average rock Sr concentrations, and $^{87}Sr/^{86}Sr$ ratios were used.

The mixing model did not work as well when considering trees as the mixture of dust and bedrock due to differences in the nature of Sr concentration of trees (woody material) versus dust or soil (minerals). The model predicted an $^{87}Sr/^{86}Sr$ ratio of trees growing over quartzite to be 0.71820, while the measured $^{87}Sr/^{86}Sr$ ratio is 0.71173 (a difference of .006). For trees over granodiorite, the model predicted an $^{87}Sr/^{86}Sr$ ratio of 0.71038, while the measured value was 0.71084 (a difference of .0004). While the predictions are not dissimilar to those for soil, the differences between Sr content in trees or bedrock and soil render this model inadequate.

3.8. Dust chronology in tree core

One core, from a tree growing over quartzite, sectioned into five-ring sections, spanning 75 rings, was analyzed to examine Sr changes over time (Table 7). The Sr isotopic ratio increased over time, from around 0.71180 to a peak of 0.71217 in modern times (Fig. 6). Large departures from the overall trends of Sr isotopic ratio and concentration exist as well. In the first half of the tree's life, $^{87}Sr/^{86}Sr$ ratios were below 0.71197, while in the second half, the ratios rose above this value. These trends produce two zones of Sr isotopic signature for this tree. The high $^{87}Sr/^{86}Sr$ ratio of this core relative to tree cores taken from trees over other bedrock types is likely due to a small contribution of Sr from the quartzite bedrock, which has a higher isotopic ratio than the dust.

4. Discussion

The goal of this work was to evaluate the use of Sr in tree rings to record dust deposition over time in the Wasatch Mountains. To this end, we characterized the $^{87}Sr/^{86}Sr$ and Sr concentration of atmospherically deposited dust and bedrock as endmembers for mixtures of soil and tree rings. Mixing model calculations suggest that dust is the major source of Sr to soil and trees, particularly those over Sr poor bedrocks, and that tree rings record the dust isotopic signal.

Different dust events with different sources feature different Sr signals. Spatially, deposited dust tends to be relatively homogeneous, although perhaps mixing of the dust cloud in the atmosphere can be more or less complete depending on atmospheric conditions and transport distance. Less complete mixing of the dust cloud in the atmosphere would cause spatial variations in dust Sr isotope ratios and concentrations. It is likely that for a given dust event, more sources were activated than were identified in this study. A dust cloud must be very large to be visible in MODIS imagery (spatial resolution from 250 to 1000 m) (NASA). Smaller

Table 7
Strontium concentration and $^{87}Sr/^{86}Sr$ ratio measurements of tree core back in time. Each core section is comprised of five consecutive rings. General ring width patterns were compared to other tree cores from the same sample site, but this core was not compared to a master chronology. The uncertainty of the Sr concentration is based on a standard uncertainty multiplied by a coverage factor $k = 2$, providing a level of confidence of approximately 95%. The error on the $^{87}Sr/^{86}Sr$ measurement is the standard error of multiple isotope ratio measurements.

Core section (approximate years)	Sr (µg/g)	$^{87}Sr/^{86}Sr$
1 (2007–2012)	5.3 (0.2)	0.71202 (0.00001)
2 (2002–2006)	7.3 (0.1)	0.71218 (0.00001)
3 (1997–2001)	6.5 (0.1)	0.71215 (0.00002)
4 (1992–1996)	6.7 (0.1)	0.71215 (0.00002)
5 (1988–1991)	7.1 (0.1)	0.71211 (0.00002)
6 (1983–1987)	5.2 (0.6)	0.71218 (0.00001)
7 (1977–1982)	7.1 (0.1)	0.7121 (0.00001)
8 (1972–1976)	8.1 (0.1)	0.71208 (0.00002)
9 (1967–1971)	8.3 (0.1)	0.71195 (0.00001)
10 (1962–1966)	8.7 (0.06)	0.71185 (0.00002)
11 (1957–1961)	9.08 (0.08)	0.71185 (0.00001)
12 (1952–1956)	10.17 (0.06)	0.71184 (0.00002)
13 (1947–1951)	7.39 (0.06)	0.71188 (0.00002)
14 (1942–1946)	10.49 (0.08)	0.71181 (0.00002)
15 (1337–1941)	7.13 (0.06)	0.71184 (0.00002)

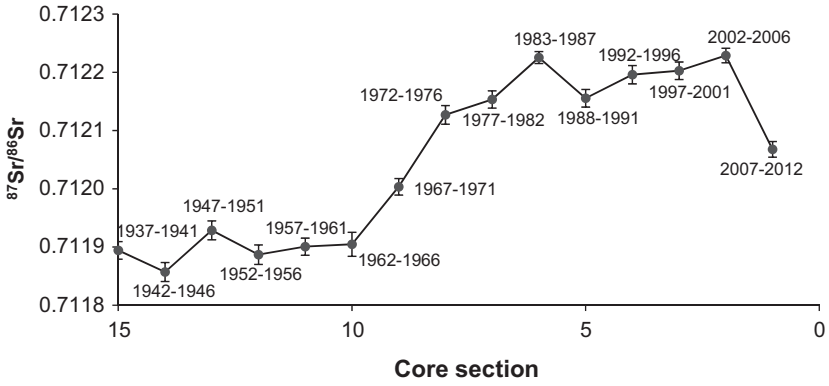

Fig. 6. $^{87}Sr/^{86}Sr$ changes in a tree core over time. Each core section includes five consecutive rings from the core of a tree growing over quartzite bedrock. $^{87}Sr/^{86}Sr$ changes are within range of values found for dust.

dust plumes originating from many areas may contribute significantly to dust deposition but be difficult to detect. The variation in dust source Sr isotopes makes Sr a useful tracer of dust sources.

The similarity of Sr between two cores from the same tree indicates that the Sr isotopic ratio in tree rings reflected the Sr source well. The analysis of natural heterogeneity of Sr in tree cores suggests that tree cores are robust records and that natural heterogeneity is not a major impediment to their use as dust proxies. Although these results support the hypothesis that Sr isotopic ratios in trees can indicate dust sources, they also indicate that estimating dust and bedrock contributions to vegetation using two-component mixing models is complex due to differences in the nature of concentrations between woody matter and soil or bedrock.

Dust is a major source of Sr for soils and trees over Sr poor bedrocks. Consistent with findings of Lawrence et al. (2011) and Lawrence et al. (2013) in the San Juan Mountains, dust supplied more weatherable material to soils, than the underlying bedrock. Several factors may contribute to trees sourcing their Sr from dust, particularly for the quartzite and granodiorite systems. Trees growing on quartzite and granodiorite may get most of their Sr from dust because there is very little Sr in quartzite or granodiorite. Additionally, dust is a more easily weathered, bioavailable source of Sr than quartzite or granodiorite.

Still, the bedrock does contribute some Sr to soil and trees, particularly limestone. Trees growing on limestone may not get as much Sr from dust because the limestone is an easily weathered source of abundant Sr that may overwhelm the dust signal. Trees growing over rapidly weathering bedrock will see more of a chemical influence from the bedrock than trees growing over slowly weathering bedrock (Cutter and Guyette, 1993).

Trees growing on quartzite and granodiorite are likely more useful than trees growing on limestone for observing changes in dust sources because neither the quartzite nor the granodiorite contributes much Sr. The greater contribution of limestone bedrock to soil and trees reduces the sensitivity of the tree to the dust signal. Despite variable Sr concentrations in bedrock and soil, Sr concentrations in trees did not vary much, suggesting that Sr uptake rates are similar among trees and that soil Sr concentration does not affect uptake amounts. Trees growing in shallow soils will also be more sensitive to atmospheric inputs due to the high ratio of land surface to volume (Cutter and Guyette, 1993).

Given that trees over quartzite and granodiorite record a dust signal, if we consider the trees as a mixture of bedrock and dust, Eq. (2) can be solved to calculate the $^{87}Sr/^{86}Sr$ ratios of dust at different times. However, we do not have a robust method to predict the dust Sr concentration in the past. Additionally, considering the trees as a mixture of bedrock and dust was not a quality model. The model was very sensitive to concentration changes, particularly within the range of Sr concentrations measured, in predicting $^{87}Sr/^{86}Sr$ ratios. As the dust Sr concentration increases, the $^{87}Sr/^{86}Sr$ ratios become less sensitive. Further, the tree could begin sourcing more Sr from the bedrock as it grows. These issues complicate the interpretation of the dust record contained within tree rings.

A potential resolution to this issue is to test the slope of the Sr isotopic ratio over time in multiple cores growing over multiple bedrock types. A parallel trend, regardless of bedrock type would indicate that the changes are due to changes in dust over time. A bedrock dependent trend, where each tree moves closer to its bedrock source would indicate that the tree is changing Sr sources throughout its lifetime from more dust as a young tree to more bedrock as the tree ages. These are valid considerations if we assume that the soil solution is at calcite saturation, and that the uptake rate of Sr by trees has been constant over time. These assumptions result in a constant input from bedrock weathering over time, making any changes in the Sr in trees due to changes in dust. Selecting trees growing over Sr poor bedrocks will also improve resolution of the dust signal.

We do not need to invoke a dust source not currently observed to explain the observed trend in Sr isotopes in tree rings over time. More likely, the relative contribution of current dust sources has changed over time. The $^{87}Sr/^{86}Sr$ ratio of the core back in time were all well within the range of $^{87}Sr/^{86}Sr$ ratios for the same five rings in different trees. However, the fact that the average ratios (samples average five rings) change over time suggests that the dominant source and the relative contributions of different sources have changed over time. Over time, the dominant sources of dust have changed. These changes likely have anthropogenic causes related to land use (Neff et al., 2008; Reynolds et al., 2010). The trend of Sr isotopes over time observed in the Wasatch Mountain core differs from the trend observed in spruce tree cores from a forest affected by acid atmospheric deposition in France (Stille et al., 2012). The tree ring $^{87}Sr/^{86}Sr$ ratios increase over time in the core from the Wasatch Mountains, while they decreased over time in the core from France. This is a reasonable difference because acid atmospheric deposition such as acid rain is likely a more significant issue in France than Utah (USGS, 2012).

The $^{87}Sr/^{86}Sr$ deposited in woody tissue should be representative of the $^{87}Sr/^{86}Sr$ ratios in the available cationic pool in the soil at a given time, and as this pool changes, so would the respective tree ring $^{87}Sr/^{86}Sr$ ratio (Gosz et al., 1983). The trees should record the soil chemistry changes in near real-time. Tulip trees showed increases in Fe and Cl concentration synchronous with active groundwater contamination (Vroblesky and Yanosky, 1990). Graustein and Armstrong (1983) argue that the similarity in Sr isotopic ratios of sapwood, bark, soil litter, and soil solution at their

study site provide evidence of rapid homogenization of Sr from both atmospheric deposition and weathering of bedrock through botanical nutrient-cycling processes. The signal provided by changing soil chemistry during ring formation is not necessarily subject to large time lags, (seasonal to annual variations can be detected).

However, soil-vegetative processes are not simple, unchanging mixtures at all time scales. Stewart et al. (1998) categorizes these processes as either steady state (isotopic ratios have reached equilibrium and do not change over time) or time dependent (isotopic ratios change over time). While the trees may record the soil chemistry in almost real time, the changes in the soil signal may occur rapidly or slowly, depending on a variety of factors that affect soil solution chemistry including dust flux, soil pH and composition, climate, and weathering rates. Over time, vegetation will cycle labile cations but this will not change the isotopic composition (Stewart et al., 1998). Time-dependent modeling of soil and tree ring changes would contribute to a more complete characterization of historical dust trends (Stewart et al., 1998).

Elemental mobility within a tree is problematic for inferring historical environmental chemistry changes from tree rings. Elements may translocate within a tree, depending on the environment, xylem characteristics of specific tree species, and element characteristics (Cutter and Guyette, 1993). Some studies have found tree rings to be poor records of elemental changes over time due to this translocation (Barnes, 1976; Hagemeyer, 2000; Zayed, 1992). Element mobility is a function of ion solubility, sapwood–heartwood equilibrium concentrations, charge/ionic radius ratio, essential nature (how essential the element is to the tree), sap pH, and chemical bonding in the xylem matrix (Cutter and Guyette, 1993). Essential elements, such as phosphorous, can be transported from interior rings to outer rings to meet the metabolic needs of the cambium (Speer, 2010). Within an annual ring, strontium has been found to gradually increase from earlywood (wood formed in the spring) to latewood (wood formed in the summer and fall) (Silkin and Ekimova, 2012) and so an annual record is preserved.

We do not believe that the change in the Sr isotopic ratio over time is related to elemental mobility within the tree. Although only one core has been analyzed, Legge et al. (1984) argue that conifers record environmental signals better than hardwoods due to the primitive nature of the wood. They note that conifers poses tracheids and only a few ray cells, as opposed to hardwoods, which possess vessels and many medium to long ray cells, which facilitate elemental translocation. Fewer ray cells should reduce translocation.

Further, several studies have addressed Sr elemental movement in plants. On a short time scale (32 days), no significant redistribution of Sr was observed in red kidney bean plants despite a high Sr concentration gradient (Rediske and Selders, 1953). Further, strontium was found to be only moderately mobile between active tree rings (rings created within the previous 1–7 years) (Padilla and Anderson, 2002) and multiyear average values may still be preserved. The time scale of translocation is poorly defined. Some researchers claim that strontium does not translocate (English et al., 2001). However, Speer (2010) found that the time scale for translocation is on the order of 3–20 years, and so the general trend in $^{87}Sr/^{86}Sr$ remains. While the analysis of an individual tree ring may not pinpoint a specific year of environmental change, trees still lend themselves to the study of broad environmental changes.

5. Conclusion

Researchers have begun to develop a deeper understanding of the role dust plays in ecological and hydrological systems, and developing a record of dust deposition is an integral part of this process. We have identified that dust was the major source of Sr in soils and trees at our study site in the Wasatch Mountains when bedrocks had low Sr concentrations. The Sr-poor bedrocks contributed very little Sr to the overlying soils and trees. Although other studies have confirmed that tree rings record chemical changes in soils (Åberg, 1995; Åberg et al., 1990; Poszwa et al., 2003; Stille et al., 2012), those changes have been due to soil acidification. We have established that at our study site in the Wasatch Mountains, trees over Sr-poor bedrocks record a dust Sr isotopic signal that can be used to understand changes in dust sources over time

These findings agree with work done in other locations including Chaco Canyon, the Sangre de Christo Mountains, and El Malpais National Monument, New Mexico (English et al., 2001; Graustein and Armstrong, 1983; Reynolds et al., 2012). Graustein and Armstrong (1983) found that over 75% of the Sr in a forested watershed in the Sangre de Christo Mountains was derived from atmospherically deposited dust. English et al. (2001) found little variation in $^{87}Sr/^{86}Sr$ ratios in modern trees growing over different bedrock types, which they attribute to the influence of dust. Reynolds et al. (2012) found that plants growing over limestone bedrocks obtained the most Sr from their substrate, while plants growing on a Precambrian gneiss or Mesozoic sandstone obtained most of their Sr from dust.

The mixing model calculations show that a majority of the Sr in soil and tree rings over quartzite and granodiorite is from atmospheric deposition. While studies of different locations have found that tree rings record other environmental processes and geochemical properties, at this site dust is clearly the major contributor of Sr to these soil and trees.

Over the past 75 years a tree growing over quartzite, with minimal Sr input from bedrock, showed a fundamental shift in the average Sr isotope ratio. Because the shift is within the range of dust ratios measured over one year, the shift can be explained by changes in the relative contribution of different sources over time without invoking a new dust source. If the dominant source of dust varied randomly from year to year or if the tree were simply recording random Sr isotope ratios, the change in ratios over time would not follow the regular trend observed. Additionally, each sample is an average of five years of dust deposition, and so changes in the average Sr isotopic ratio are more robust than annual variations.

Our findings suggest that using mixing models to understand past dust deposition involves additional complexity related to the soil and bedrock contribution of Sr. Trees growing over a Sr-poor bedrock such as the Tintic Quartzite record a time-averaged loading of dust with very little contribution from bedrock and should be used in future work. The time averaging is due to the annual growth of tree rings, as well as soil mixing processes. Thus the trees show general trends. The Sr isotope signature of a soil in a given year is ultimately a mixture of all prior and immediate atmospheric deposition, as well as bedrock. Questions on the influence of local conditions such as soil moisture, composition, and formation, root depth, or groundwater on the Sr isotopic signal resolution remain, as do questions on the specifics of vegetative uptake of elements like Sr. Future work should focus on refining the dust Sr signal, validating this tool on a larger scale including more trees over a longer time period, as well as developing a dust source map including the Sr concentration and isotope ratio of different source areas.

Acknowledgements

We thank the reviewers for their thoughtful input, which greatly improved the manuscript. We acknowledge the use of

Rapid Response imagery from the Land Atmosphere Near-real time Capability for EOS (LANCE) system operated by the NASA/GSFC/Earth Science Data and Information System (ESDIS) with funding provided by NASA/HQ. Thank you to Chris Anderson and Shawn Thomas for help in the lab, David Coyne and Fletcher Reed for their help with fieldwork, Scott Hynek and Glen Mackey for their intellectual input, and Blake Wellard and Mitch Powers for their insight into dendrochronology. Funding was provided through the University of Utah Geology and Geophysics Graduate Student Research Fund. A University of Utah Global Change and Sustainability Center Fellowship supported Olivia Miller.

References

Åberg, G., 1995. The use of natural strontium isotopes as tracers in environmental studies. Water Air Soil Pollut. 79, 309–322.

Åberg, G., Jacks, G., Wickman, T., Hamilton, P.J., 1990. Strontium isotopes in trees as an indicator for calcium availability. CATENA 17, 1–11.

Alexander, Robert R., Shepperd, Wayne D., 2004. *Picea engelmannii* Parry ex Engelm., Engelmann Spruce, Silvics Manual, vol. 1. USDA Forest Service. <http://www.na.fs.fed.us/pubs/silvics_manual/Volume_1/picea/engelmannii.htm>.

Barnes, D., 1976. The lead, copper and zinc content of tree rings and bark. A measurement of local metallic pollution. Sci. Total Environ. 5, 63–67.

Baruah, B.K., Das, B., Haque, A., Medhi, C., Misra, A.K., 2011. Sequential extraction of common metals (Na, K, Ca and Mg) from surface soil. J. Chem. Pharm. Res. 3, 565–573.

Belnap, J., Gillette, D.A., 1997. Disturbance of biological soil crusts: impacts on potential wind erodibility of sandy desert soils in southeastern Utah. Land Degrad. Dev. 8, 355–362.

Beramendi-Orosco, L.E., Rodriguez-Estrada, M.L., Morton-Bermea, O., Romero, F.M., Gonzalez-Hernandez, G., Hernandez-Alvarez, E., 2013. Correlations between metals in tree-rings of *Prosopis julifora* as indicators of sources of heavy metal contamination. Appl. Geochem. 39, 78–84.

Bowen, H., Dymond, J., 1956. The uptake of calcium and strontium by plants from soils and nutrient solutions. J. Exp. Bot. 7, 264–272.

Bryant, B., 1990. Geologic Map of the Salt Lake City 30′ × 60′ Quadrangle, North-Central Utah, and Uinta County, Wyoming. In: Survey, U.G. (Ed.), Miscellaneous Investigations Series, Map I-1944 ed.

Capo, R.C., Chadwick, O.A., 1999. Sources of strontium and calcium in desert soil and calcrete. Earth Planet. Sci. Lett. 170, 61–72.

Capo, R.C., Stewart, B.W., Chadwick, O.A., 1998. Strontium isotopes as tracers of ecosystem processes: theory and methods. Geoderma 82, 197–225.

Carling, G.T., Fernandez, D.P., Johnson, W.P., 2012. Dust-mediated loading of trace and major elements to Wasatch Mountain snowpack. Sci. Total Environ. 432, 65–77.

Chiquet, A., Michard, A., Nahon, D., Hamelin, B., 1999. Atmospheric input vs in situ weathering in the genesis of calcretes: an Sr isotope study at Galvez (Central Spain). Geochim. Cosmochim. Acta 63, 311–323.

Cutter, B.E., Guyette, R.P., 1993. Anatomical, chemical, and ecological factors affecting tree species choice in dendrochemistry studies. J. Environ. Qual. 22, 611–619.

Dart, R.C., Wittwer, P.D., Barovich, K.M., Chittleborough, D.J., Hill, S.M., 2004. Strontium isotopes as an indicator of the source of calcium for regolith carbonates. In: Roach, I.C. (Ed.), Regolith. CRC LEME, Adelaide, South Australia, pp. 67–70.

Draxler, R.R., Rolph, G.D., 2012. HYSPLIT (HYbrid Single-Particle Lagrangian Integrated Trajectory). NOAA Air Resources Laboratory, Silver Spring, MD. Model Access via NOAA ARL READY Website <http://ready.arl.noaa.gov/HYSPLIT.php>.

Drouet, T., Herbauts, J., Demaiffe, D., 2005. Long-term records of strontium isotopic composition in tree rings suggest changes in forest calcium sources in the early 20th century. Global Change Biol. 11, 1926–1940.

Eghbal, M.K., 1993. Stratigraphy and genesis of Durorthids and Haplargids on dissected alluvial fans, western Mojave Desert, California. Geoderma 59, 151–174.

Eldridge, D.J., Leys, J.F., 2003. Exploring some relationships between biological soil crusts, soil aggregation and wind erosion. J. Arid Environ. 53, 457–466.

Engelbrecht, J.P., Derbyshire, E., 2010. Airborne mineral dust. Elements 6, 241–246.

English, N.B., Betancourt, J.L., Dean, J.S., Quade, J., 2001. Strontium isotopes reveal distant sources of architectural timber in Chaco Canyon, New Mexico. Proc. Natl. Acad. Sci. 98, 11891–11896.

Faure, G., 1977. Strontium Isotope Geology. John Wiley and Sons Inc., New York, NY.

Field, J.P., Belnap, J., Breshears, D.D., Neff, J.C., Okin, G.S., Whicker, J.J., Painter, T.H., Ravi, S., Reheis, M.C., Reynolds, R.L., 2009. The ecology of dust. Frontiers Ecol. Environ. 8, 423–430.

Gerloff, G.C., Moore, D.G., Curtis, J.T., 1966. Selective absorption of mineral elements by native plants of Wisconsin. Plant Soil 25, 393–405.

Gosz, J.R., Brookins, D.G., Moore, D.I., 1983. Using strontium isotope ratios to estimate inputs to ecosystems. BioScience 33, 23–30.

Graustein, W.C., Armstrong, R.L., 1983. The use of strontium-87/strontium-86 ratios to measure atmospheric transport into forested watersheds. Science 219, 289–292.

Grousset, F.E., Biscaye, P.E., 2005. Tracing dust sources and transport patterns using Sr, Nd and Pb isotopes. Chem. Geol. 222, 149–167.

Hagemeyer, J., 2000. Trace metals in tree rings: what do they tell us? In: Markert, B., Friese, K. (Eds.), Trace Metals in the Environment. Elsevier, pp. 375–385 (Chapter 13).

Hahnenberger, M., Nicoll, K., 2012. Meteorological characteristics of dust storm events in the eastern Great Basin of Utah, USA. Atmos. Environ. 60, 601–612.

James, Larry P., Crittenden Jr., Max D., Calkins, Frank C., Sharp, Byron J., Baker, Arthur A., Bromfield, Calvin S., 1978. Geology of Big Cottonwood Mining District, Plate 1, Bulletin 114. Utah Geological Survey, State of Utah Department of Natural Resources.

Lawrence, C.R., Painter, T.H., Landry, C.C., Neff, J.C., 2010. Contemporary geochemical composition and flux of aeolian dust to the San Juan Mountains, Colorado, United States. J. Geophys. Res. 115, G03007.

Lawrence, C.R., Neff, J.C., Farmer, G.L., 2011. The accretion of aeolian dust in soils of the San Juan Mountains, Colorado, USA. J. Geophys. Res.: Earth Surf. 116, F02013.

Lawrence, C.R., Reynolds, R.L., Ketterer, M.E., Neff, J.C., 2013. Aeolian controls of soil geochemistry and weathering fluxes in high-elevation ecosystems of the Rocky Mountains, Colorado. Geochim. Cosmochim. Acta 107, 27–46.

Legge, A.H., Kaufmann, H.C., Winchester, J.W., 1984. Tree-ring analysis by PIXE for a historical record of soil chemistry response to acidic air pollution. Nucl. Instrum. Methods Phys. Res., Sect. B 3, 507–510.

Lindgren, W., Loughlin, G.F., Heikes, V.C., 1919. Geology and Ore Deposits of the Tintic Mining District, Utah, with a Historical Review, USGS Professional Paper.

Mackey, G.N., Fernandez, D., 2011. High through-put Sr Isotope Analysis using an Automated Column Chemistry System. American Geophysical Union, Poster Presented at the 2011 Fall Meeting, San Francisco, CA.

Miller, M.E., Bowker, M.A., Reynolds, R.L., Goldstein, H.L., 2012. Post-fire land treatments and wind erosion – lessons from the Milford Flat Fire, UT, USA. Aeolian Res. 7, 29–44.

NASA, MODIS Specifications. <http://modis.gsfc.nasa.gov/about/specifications.php> (accessed 05.21.14).

NASA/GSFC/Earth Science Data and Information System, E., Land Atmosphere Near-real time Capability for EOS (LANCE) System.

Neff, J., Ballantyne, A., Farmer, G., Mahowald, N., Conroy, J., Landry, C., Overpeck, J., Painter, T., Lawrence, C., Reynolds, R., 2008. Increasing eolian dust deposition in the western United States linked to human activity. Nat. Geosci. 1, 189–195.

Oviatt, C.G., 1997. Lake Bonneville fluctuations and global climate change. Geology 25, 155–158.

Padilla, K.L., Anderson, K.A., 2002. Trace element concentration in tree-rings biomonitoring centuries of environmental change. Chemosphere 49, 575–585.

Painter, T.H., Barrett, A.P., Landry, C.C., Neff, J.C., Cassidy, M.P., Lawrence, C.R., McBride, K.E., Farmer, G.L., 2007. Impact of disturbed desert soils on duration of mountain snow cover. Geophys. Res. Lett. 34, L12502.

Painter, T.H., Deems, J.S., Belnap, J., Hamlet, A.F., Landry, C.C., Udall, B., 2010. Response of Colorado River runoff to dust radiative forcing in snow. Proc. Natl. Acad. Sci. 107, 17125–17130.

Poszwa, A., Wickman, T., Dambrine, E., Ferry, B., Dupouey, J., Helle, G., Schleser, G., Breda, N., 2003. A retrospective isotopic study of spruce decline in the Vosges Mountains (France). Water Air Soil Pollut.: Focus 3, 201–222.

Rabenhorst, M.C., 1984. Airborne dusts in the Edwards Plateau Region of Texas. Soil Sci. Soc. Am. J. 48, 521–627.

Rediske, J., Selders, A., 1953. The absorption and translocation of strontium by plants. Plant Physiol. 28, 594.

Reynolds, R., Mordecai, J., Rosenbaum, J., Ketterer, M., Walsh, M., Moser, K., 2010. Compositional changes in sediments of subalpine lakes, Uinta Mountains (Utah): evidence for the effects of human activity on atmospheric dust inputs. J. Paleolimnol. 44, 161–175.

Reynolds, A.C., Quade, J., Betancourt, J.L., 2012. Strontium isotopes and nutrient sourcing in a semi-arid woodland. Geoderma 189–190, 574–584.

Reynolds, R.L., Goldstein, H.L., Moskowitz, B.M., Bryant, A.C., Skiles, S.M., Kokaly, R.F., Flagg, C.B., Yauk, K., Berquó, T., Breit, G., Ketterer, M., Fernandez, D., Miller, M.E., Painter, T.H., 2013. Composition of dust deposited to snow cover in the Wasatch Range (Utah, USA): Controls on radiative properties of snow cover and comparison to some dust-source sediments. Aeolian Res. http://dx.doi.org/10.1016/j.aeolia.2013.08.001.

Ricker, W.E., 1973. Linear regression in fishery research. J. Fish. Res. Board Can., 409–434.

Roca, M.C., Vallejo, V.R., 1995. Effect of soil potassium and calcium on caesium and strontium uptake by plant roots. J. Environ. Radioact. 28, 141–159.

Silkin, P.P., Ekimova, N.V., 2012. Relationship of strontium and calcium concentrations with the parameters of cell structure in Siberian spruce and fir tree-rings. Dendrochronologia 30, 189–194.

Speer, J., 2010. Fundamentals of Tree-ring Research. The University of Arizona Press, Tuscon.

Steenburgh, J.W., Massey, J.D., Painter, T.H., 2012. Episodic dust events of Utah's Wasatch Front and adjoining region. J. Appl. Meterol. Climatol. 51, 1654–1669.

Stewart, B.W., Capo, R.C., Chadwick, O.A., 1998. Quantitative strontium isotope models for weathering, pedogenesis and biogeochemical cycling. Geoderma 82, 173–195.

Stille, P., Schmitt, A.-D., Labolle, F., Pierret, M.-C., Gangloff, S., Cobert, F., Lucot, E., Guéguen, F., Brioschi, L., Steinmann, M., Chabaux, F., 2012. The suitability of annual tree growth rings as environmental archives: evidence from Sr, Nd, Pb and Ca isotopes in spruce growth rings from the Strengbach watershed. C. R. Geosci. 344, 297–311.

Stokes, M.A., 1996. An Introduction to Tree-ring Dating. University of Arizona Press.
Tessier, A., 1979. Sequential extraction procedure for the speciation of particulate trace metals. Anal. Chem. 51, 844–851.
USEPA, 1996. USEPA Method 3050, 1996. Acid Digestion of Sediments, Sludges, and Soils.
USGS, 2012. Acid Rain, Atmosperic Deposition, and Precipitation Chemistry.
Van der Hoven, S.J., Quade, J., 2002. Tracing spatial and temporal variations in the sources of calcium in pedogenic carbonates in a semiarid environment. Geoderma 108, 259–276.
Vogel, T.A., Cambray, F.W., Constenius, K.N., 2001. Origin and emplacement of igneous rocks in the central Wasatch Mountains, Utah. Rocky Mountain Geol. 36, 119–162.
Vroblesky, D.A., Yanosky, T.M., 1990. Use of tree-ring chemistry to document historical ground-water contamination events. Ground Water 28, 677–684.
West, L.T., 1988. Calciustolls in central Texas: II. Genesis of calcic and petrocalcic horizons. Soil Sci. Soc. Am. J. 52, 1731–1740.
Zayed, J., 1992. Variations of trace element concentrations in red spruce tree rings. Water Air Soil Pollut. 65, 281–291.
Zobitz, J.M., Keener, J.P., Schnyder, H., Bowling, D.R., 2006. Sensitivity analysis and quantification of uncertainty for isotopic mixing relationships in carbon cycle research. Agric. For. Meteorol. 136, 56–75.